

Application of Ionic Liquids Containing Tricyanomethanide $[\text{C}(\text{CN})_3]^-$ or Tetracyanoborate $[\text{B}(\text{CN})_4]^-$ Anions in Dye-Sensitized Solar Cells

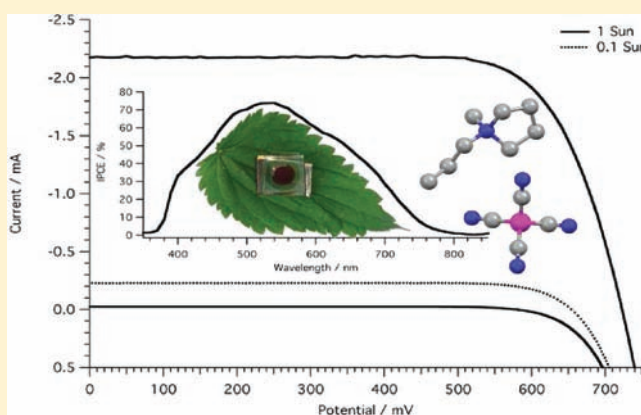
Magdalena Marszalek,[†] Zhaofu Fei,[†] Dun-Ru Zhu,[‡] Rosario Scopelliti,[†] Paul J. Dyson,^{*,†} Shaik Mohammed Zakeeruddin,^{*,†} and Michael Grätzel[†]

[†]Institut des Sciences et Ingénierie Chimiques, Ecole Polytechnique Fédérale de Lausanne (EPFL), CH-1015 Lausanne, Switzerland

[‡]State Key Laboratory of Materials-Oriented Chemical Engineering, College of Chemistry and Chemical Engineering, Nanjing University of Technology, Nanjing 210009, P. R. China

Supporting Information

ABSTRACT: A series of novel ionic liquids composed of imidazolium, pyridinium, pyrrolidinium, and ammonium cations with tricyanomethanide or tetracyanoborate anions were prepared. The ionic liquids were characterized by NMR and IR spectroscopy and ESI-mass spectrometry, and their physical properties were investigated. Solid state structures of the N-propyl-N-methylpyrrolidinium and triethylpropylammonium tetracyanoborate salts were obtained by single crystal X-ray diffraction. The salts that are liquid at room temperature were evaluated as electrolyte additives in dye-sensitized solar cells, giving rise to efficiencies 7.35 and 7.85% under 100 and 10% Sun, respectively, in combination with the standard Z907 dye.



INTRODUCTION

Despite the ongoing interest in ionic liquids (ILs),^{1,2} the majority of the research is based on ILs containing a rather limited set of fluorine-containing anions, notably tetrafluoroborate (BF_4^-), hexafluorophosphate (PF_6^-), and bis-(trifluoromethylsulfonyl)imide (Tf_2N^-).³ In contrast, ILs based on nonfluorous anions, i.e., tricyanomethanide ($[\text{C}(\text{CN})_3]^-$)^{4–6} and tetracyanoborate ($[\text{B}(\text{CN})_4]^-$),^{7,8} are somewhat underexplored. Indeed, it has been reported that ILs with $[\text{C}(\text{CN})_3]^-$ and $[\text{B}(\text{CN})_4]^-$ anions have low viscosities.^{4,8} For example, $[\text{EMI}][\text{C}(\text{CN})_3]$ (where EMI = 1-ethyl-3-methylimidazolium cation) has a viscosity of 18 cP at 22 °C and a melting point of 11 °C,⁴ and $[\text{EMI}][\text{B}(\text{CN})_4]$ has a viscosity of 19 cP at 21 °C,⁸ both being lower than that of $[\text{EMI}][\text{Tf}_2\text{N}]$, 27 cP at 20 °C.⁹ N,N,N',N'-Tetramethyl-N'',N''-dipentylguanidinium tricyanomethanide has a viscosity of 88 cP,⁶ the value being relatively low given the cation.

There are only a limited numbers of ILs that contain $[\text{C}(\text{CN})_3]^-$ and $[\text{B}(\text{CN})_4]^-$ anions and their applications have been scarcely explored, despite the high stability and interesting electrochemical and physicochemical properties of the $[\text{B}(\text{CN})_4]^-$ anion.¹⁰ Indeed, in nearly all of the applications, including electrolytes,^{11–13} as well as others,^{14,15} studies are almost exclusively on the $[\text{EMI}]^+$ -based systems.

In this paper, the synthesis and characterization of a series of new ILs with $[\text{C}(\text{CN})_3]^-$ and $[\text{B}(\text{CN})_4]^-$ anions are described.

Some of the room temperature ILs were employed as electrolytes in dye-sensitized solar cells giving very good efficiencies exceeding 7%.

RESULTS AND DISCUSSION

The preparation of ILs with BF_4^- , PF_6^- , and Tf_2N^- anions is well established,^{16,17} whereas there are relatively few reports describing the synthesis of ILs with $[\text{C}(\text{CN})_3]^-$ anions. The synthesis of ILs with $[\text{B}(\text{CN})_4]^-$ anions is only covered in a patent, and details of the anion exchange of the alkali metal salts of tetracyanoborate with imidazolium or pyridinium halides have not been reported.⁷ In this work, we used a literature protocol to react 1-propyl-3-methylimidazolium chloride $[\text{PMI}]\text{Cl}$ with $\text{Na}[\text{C}(\text{CN})_3]$ in aqueous solution, and the resulting IL, $[\text{PMI}][\text{C}(\text{CN})_3]$ (**1a**), was extracted with dichloromethane. Similarly, reaction of $[\text{PMI}]\text{Cl}$ with $\text{K}[\text{B}(\text{CN})_4]$ gives the IL $[\text{PMI}][\text{B}(\text{CN})_4]$ (**1b**). Using the same approach, ILs containing N-propylpyridinium, N-propyl-N-methylpyrrolidinium, and triethylpropylammonium cations with the $[\text{C}(\text{CN})_3]^-$ anion (**2a–4a**) and the $[\text{B}(\text{CN})_4]^-$ anion (**2b–4b**) were prepared (see Figure 1).

The $[\text{C}(\text{CN})_3]^-$ containing ILs, **1a–4a**, are liquid at room temperature, whereas of the ILs containing the $[\text{B}(\text{CN})_4]^-$

Received: July 15, 2011

Published: October 25, 2011

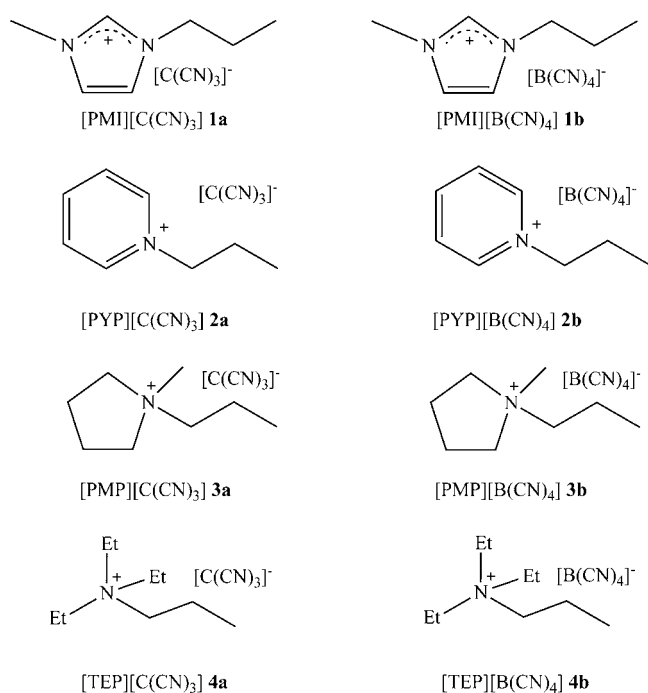


Figure 1. Structures and numbering scheme of the ILs prepared in this study.

anion, i.e., **1b–4b**, only **1b** and **2b** are liquid at room temperature. The ^1H and ^{13}C NMR spectra of **1a–4a**, **1b**, and **2b** are recorded as ILs without being dissolved in any solvent using a C_6D_6 capillary for login. Spectra of **3b** and **4b** were obtained in a CD_2Cl_2 solution (see the Experimental Section). In general, the signals do not differ much from those of the precursor salts—the variation being typical for ILs.^{18–20} The IR spectra of **1a–4a** contain absorptions between 2153 and 2164 cm^{-1} that correspond to the $\text{C}\equiv\text{N}$ bond; the absorptions lie in a rather smaller range compared to those observed in salts with metal cations.^{21–24} In **1b–4b**, the absorptions of the CN group are observed at markedly higher wavenumbers (ca. 2222 cm^{-1}) and are significantly shifted from those containing metal cations, which are found in the range of 2250 to 2290 cm^{-1} ,^{25–27} but nonetheless are close in value to those observed in tetrabutylammonium²⁸ and tetrabutylphosphonium²⁹ salts. It is known that the $\text{C}\equiv\text{N}$ absorption in salts containing $[\text{C}(\text{CN})_3]^-$ and $[\text{B}(\text{CN})_4]^-$ anions is sensitive to the structure of the cations and is susceptible to $\pi\cdots\pi$ and/or $\pi\cdots\text{H}$ noncovalent interactions.²¹

Although salts containing the tetracyanoborate anion were reported many years ago,³⁰ the structure of simple lithium salt was reported only recently,³¹ followed by the structures of potassium,³² sodium, rubidium, cesium, and ammonium salts;²⁵ several transition metal salts;^{26,27} and somewhat more exotic salts.³³ Single crystals of **3b** and **4b** were obtained by slow cooling from the liquid state from 110° to room temperature over a period of 24 h, and their structures were determined by X-ray diffraction (see the Experimental Section). Only very few salts with organic cations (e.g., tetrabutylphosphonium and tetrabutylammonium salts) have been reported,^{28,29} and the structures of **3b** and **4b** (Figure 2) represent the first examples of tetracyanoborate salts containing asymmetric cations.

In **3b** and **4b**, the anion adopts a nearly ideal tetrahedral structure with the C–B–C angles close to 109.4° and B–C–N angles close to 180°. The average C–N distance in the nitrile

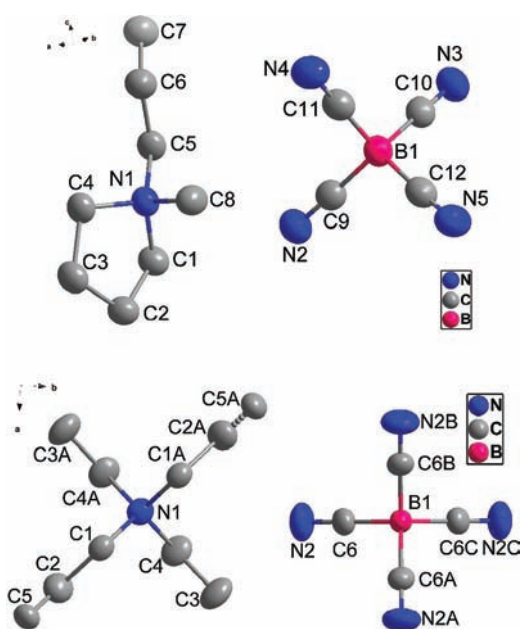


Figure 2. Solid state structures of **3b** (top) and **4b** (bottom) with the thermal ellipsoids at 50% probability and H atoms were omitted for clarity. Selected bond distances (Å) and angles (deg). **3b**: N(1)–C(5) 1.506(4), N(1)–C(1) 1.522(5), N(2)–C(9) 1.153(5), N(3)–C(10), 1.143(5), B(1)–C(10), 1.590(6), B(1)–C(11), 1.594(7), C(10)–B(1)–C(11) 109.7(3), C(10)–B(1)–C(12) 108.7(3). **4b**: N(1)–C(1) 1.518(3), N(1)–C(4) 1.522(3), N(2)–C(6) 1.143(2), B(1)–C(6) 1.5941(18), C(6)–B(1)–C(6A) 109.00(6).

groups is 1.14 Å in **3b** and **4b**, nearly the same as those observed in the lithium (1.14 Å)³¹ and potassium (1.14 Å) salts.³² These values are in the range found in the ammonium and phosphonium salts.^{28,29} In the crystal of **3b**, the anions are connected by weak hydrogen bonds forming a C–H \cdots N–C–B–C–N \cdots H–C network (Figure 3). The D \cdots A distances of the C–H \cdots N hydrogen bonds range from 3.40 to 3.53 Å (Figure 3 and Table 1). These distances are rather longer than those that exist in series of imidazolium salts with other anions such as Tf_2N^- and BF_4^- .^{34,35} The CH_3 group of the propyl substituent in **4b** is disordered, but hydrogen bonds are observed between the CH_3 group of the ethyl substituents and the anion, with the shortest (C)–H \cdots N–C distance being 2.638 Å.

The room temperature ILs **1a/b**, **2a/b**, **3a**, and **4a** were used to prepare electrolytes, and their viscosities and tri-iodide diffusion coefficients were determined. Subsequently, they were evaluated in dye-sensitized solar cells following the procedure described for the standard eutectic melt electrolyte coded Z952.¹⁴ Essentially, the new ILs were incorporated into the electrolytes in place of 1-ethyl-3-methylimidazolium tricyanomethanide $[\text{EMI}][\text{C}(\text{CN})_3]$ at the same molar ratio, giving electrolytes termed M-**1a**, M-**1b**, M-**2a**, M-**2b**, M-**3a**, and M-**4a** (see the Experimental Section).

The electrolytes with $[\text{C}(\text{CN})_3]^-$ are less viscous than their $[\text{B}(\text{CN})_4]^-$ analogues (namely M-**1a** vs M-**1b** and M-**2a** vs M-**2b**). Diffusion coefficients of I_3^- were obtained by cyclic voltammetry and electrochemical impedance spectroscopy (EIS) performed on symmetric cells, and the results obtained by these two methods are shown in Table 2. Electrolytes M-**1a** and M-**2a** have slightly higher tri-iodide diffusion coefficients, presumably due to their lower viscosity.

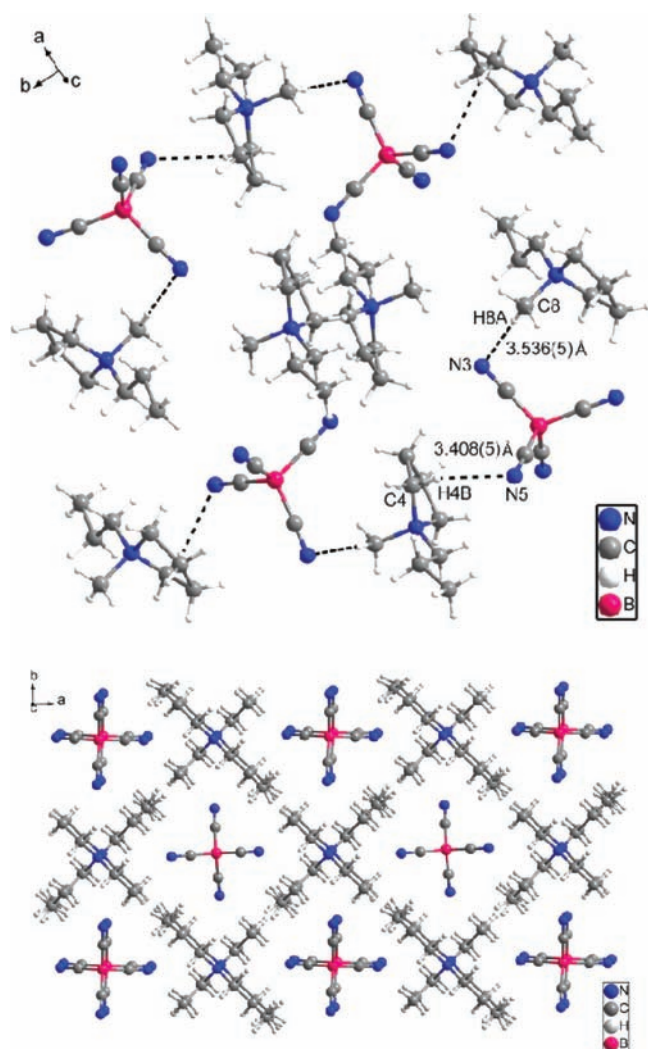


Figure 3. Crystal packing in 3b (top) and 4b (bottom).

Table 1. Principle Hydrogen Bond Parameters in 3b

| D–H...A | D–H (Å) | H...A (Å) | D...A (Å) | D–H...A (deg) |
|--------------------------|---------|-----------|-----------|---------------|
| C4–H4B...N5 ^a | 0.990 | 2.570 | 3.408(5) | 142.00 |
| C8–H8A...N3 ^b | 0.980 | 2.560 | 3.536(5) | 171.00 |

^aSymmetry code: $x, 3/2 - y, 1/2 + z$. ^bSymmetry code: $-x, 1 - y, -z$.

Table 2. Comparison of the Diffusion Coefficients of I_3^- in Electrolytes and Their Viscosities^a

| electrolyte | | M-1a | M-2a | M-3a | M-1b | M-2b |
|---|-----|------|------|------|------|------|
| $D_{I_3^-}/10^{-7} \text{ cm}^2 \text{ s}^{-1}$ | CV | 2.51 | 2.27 | 3.42 | 2.39 | 2.09 |
| | EIS | 1.66 | 1.54 | 1.82 | 1.20 | 1.27 |
| viscosity (cP at 20 °C) | | 49.8 | 49.4 | 59.1 | 56.5 | 53.0 |

^aData for M-4a is not available because it is a quasi-solid substance.

The six new electrolytes have been formulated for use in DSC devices in combination with Z907 as a sensitizer (Table 3). The best DSC device contains the electrolyte M-1a; the open-circuit voltage (V_{oc}), short-circuit current density (J_{sc}), and fill factor (FF) are 725 mV, 13.7 mA/cm², and 0.743, respectively, yielding an overall photoconversion efficiency (PCE) of 7.35% at full sunlight intensity. However, the PCE at 10% light intensity is as high as 7.85% due to diminished problems with diffusion connected with slower cell dynamics

Table 3. Photovoltaic Characteristics of the Solar Cells Measured under AM 1.5G, 100% Sun, and 10% Sun

| electrolyte | sun intensity/ % | $J_{sc}/$ mA·cm ⁻² | $V_{oc}/$ mV | fill factor | efficiency/ % |
|-------------|---------------------|----------------------------------|-----------------|----------------|------------------|
| M-1a | 100 | 13.7 | 725 | 0.743 | 7.35 |
| | 10 | 1.43 | 655 | 0.802 | 7.85 |
| M-2a | 100 | 13.6 | 710 | 0.750 | 7.2 |
| | 10 | 1.41 | 645 | 0.797 | 7.6 |
| M-3a | 100 | 12.65 | 725 | 0.722 | 6.7 |
| | 10 | 1.32 | 655 | 0.798 | 7.2 |
| M-4a | 100 | 12.2 | 725 | 0.733 | 6.5 |
| | 10 | 1.36 | 660 | 0.806 | 7.5 |
| M-1b | 100 | 14.8 | 685 | 0.714 | 7.2 |
| | 10 | 1.54 | 620 | 0.779 | 7.7 |
| M-2b | 100 | 12.7 | 700 | 0.746 | 6.6 |
| | 10 | 1.36 | 635 | 0.805 | 7.25 |

under these light conditions. The J – V curves of the device with electrolyte M-1a are presented in Figure 4. The incident

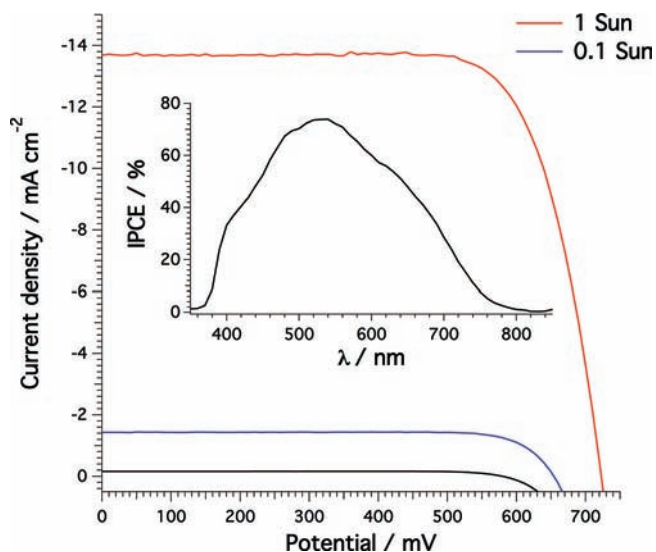


Figure 4. Current density–voltage characteristic of the device containing the electrolyte M-1a. Incident photon-to-current conversion efficiency spectrum of the same cell (inset).

photon-to-current efficiency (IPCE) of the device M-1a is shown in the inset of Figure 4. The maximum IPCE value at 550 nm is more than 70%. The DSC devices exhibit rather linear performance with an increasing intensity of irradiating light, and only a small current drop (~5%) was noticed at 1 Sun, presumably due to mass transport limitations of tri-iodide.

There is a clear trend between the open circuit potential of the DSCs and the counter ion of the IL used in the electrolyte. Electrolytes containing the $[C(CN)_3]^-$ anion exhibit higher V_{oc} values, by ~20 mV, compared to those with the $[B(CN)_4]^-$ anion. We employed transient photovoltage decay measurements on the cells with different electrolytes to compare the rate of interfacial recombination of electrons from the TiO₂ conduction band to the oxidized form of the redox mediator, tri-iodide. In Figure 5, the apparent electron lifetime calculated for cells with the different electrolytes is plotted against extracted charge, which provides a clearer comparison, because the difference between the quasi-Fermi level and the conduction band is kept constant for each measured point.

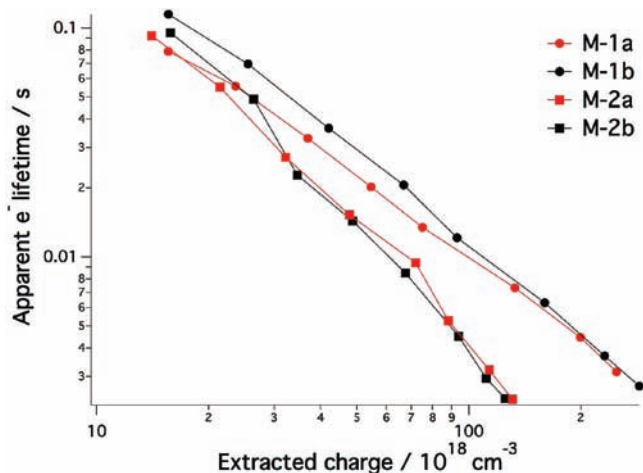


Figure 5. Apparent electron lifetimes in DSCs with electrolytes M-1a, M-1b, M-2a, and M-2b. The lines are only present to guide the eye.

The DSCs with electrolytes **1a**, **1b**, **2a**, and **2b** were compared. It appears that the two anions, $[\text{C}(\text{CN})_3]^-$ and $[\text{B}(\text{CN})_4]^-$, do not influence the recombination rate, since the electron lifetimes for the cells with electrolytes sharing the same cation are practically identical. Nevertheless, the planar $[\text{C}(\text{CN})_3]^-$ anion³⁶ could potentially facilitate access to the TiO_2 surface, as it could adsorb on it more easily than the tetrahedral $[\text{B}(\text{CN})_4]^-$ anion.³² Indeed, a more detailed comparison between the $[\text{B}(\text{CN})_4]^-$ and dicyanoamide, $[\text{N}(\text{CN})_2]^-$, anions has been reported.³⁷ It was found that $[\text{N}(\text{CN})_2]^-$ containing electrolytes have higher open circuit potential than $[\text{B}(\text{CN})_4]^-$ based electrolytes, and this difference was ascribed to suppressed interfacial charge-transfer behavior in addition to an increase in the conduction band edge position of TiO_2 due to the surface interaction with the $[\text{N}(\text{CN})_2]^-$ anion. Cell capacitance corresponds to the density of states. Difference of the open-circuit potentials at a given capacitance indicates a shift of the conduction band. While we did not observe similar differences in the recombination rates, the specific adsorption of $[\text{C}(\text{CN})_3]^-$ may be responsible for the upward shift of the conduction band of TiO_2 , especially as this difference corresponds very well with the difference between V_{oc} values of the devices (Figure 6) at a given density of states.

In conclusion, we have prepared and characterized a series of new fluorine-free ILs containing imidazolium, pyridinium, pyrrolidinium, and ammonium cations and $[\text{C}(\text{CN})_3]^-$ and $[\text{B}(\text{CN})_4]^-$ anions. These ILs were evaluated as components in dye-sensitized solar cells, and the influence of the anion was found to be negligible, giving comparable results to those containing TF_2N anions. Nevertheless, these results are likely to generate increased interest in ILs containing these anions.

EXPERIMENTAL SECTION

Imidazolium, pyridinium, pyrrolidinium, and ammonium halides were purchased from Iolitec (Germany) and used as received. Sodium tricyanomethanide $\text{Na}[\text{C}(\text{CN})_3]$ and potassium tetracyanoborate $\text{K}[\text{B}(\text{CN})_4]$ were received as a gift from Lonza AG and from Merck KGaA, respectively. IR spectra were recorded on a Perkin-Elmer FT-IR 2000 system. NMR spectra were measured on a Bruker DMX 400, using Me_4Si as an external standard. Electrospray ionization mass spectra (ESI-MS) were recorded on a ThermoFinnigan LCQ-Deca XP Plus quadrupole ion trap instrument using a literature method.³⁸ Elemental analysis was carried out at the EPFL.

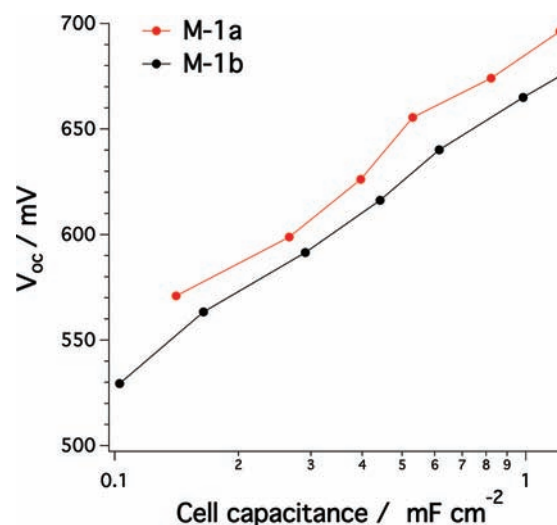


Figure 6. The upward shift of the conduction band of TiO_2 induced by the different anions present in the electrolyte in a DSC.

General Synthetic Procedure. The appropriate imidazolium, pyridinium, pyrrolidinium, or ammonium halide was mixed with $\text{Na}[\text{C}(\text{CN})_3]$ or $\text{K}[\text{B}(\text{CN})_4]$ in a molar ratio of 1:1 in water (5 mL). After stirring at room temperature for 24 h, the reaction mixture was extracted with dichloromethane (3×10 mL). Removal of the dichloromethane gave the desired IL that was dissolved in dry dichloromethane and then stored at -20 °C for 24 h. The solution was filtered to remove traces of sodium or potassium halide, and after removal of the solvent, the product was dried under vacuum conditions.

1a: This IL was prepared from 1-propyl-3-methylimidazolium chloride (1.61 g, 0.01 mol) and $\text{Na}[\text{C}(\text{CN})_3]$ (1.13 g, 0.01 mol). Yield: 95%. ^1H NMR (Neat, C_6D_6 capillary): 9.00 (s, 1H), 7.80 (s, 1H), 7.75 (s, 1H), 4.50 (t, 2H, $J(\text{HH}) = 6.50$ Hz), 4.20 (s, 3H), 2.20 (m, 2H), 1.25 (t, 3H, $J(\text{HH}) = 6.50$ Hz). ^{13}C NMR (Neat, C_6D_6 capillary): 136.5, 123.5, 122.5, 121.4, 51.6, 36.0, 24.5, 11.0, 6.1. IR (cm^{-1}): 3114, 2970, 2164, 1573, 1456, 1169, 1066, 892. ESI-MS (CH_3CN) (m/z), positive ion: 125 [cation]⁺. Negative ion: 90 $[\text{C}(\text{CN})_3]^-$. Anal. Calcd for $\text{C}_{11}\text{H}_{13}\text{N}_5$ (215.26): C, 61.38; H, 6.09; N, 32.53%. Found: C, 61.29; H, 6.07; N, 32.56%.

1b: This IL was prepared from 1-propyl-3-methylimidazolium chloride (1.00 g, 0.006 mol) and $\text{K}[\text{B}(\text{CN})_4]$ (0.96 g, 0.006 mol). Yield: 97%. ^1H NMR (neat, C_6D_6 capillary): 9.00 (s, 1H), 7.96 (s, 1H), 7.92 (s, 1H), 4.70 (t, 2H, $J(\text{HH}) = 6.50$ Hz), 4.45 (s, 3H), 2.45 (m, 2H), 1.50 (t, 3H, $J(\text{HH}) = 6.50$ Hz). ^{13}C NMR (neat, C_6D_6 capillary): 137.0, 123.5, 123.0, 122.2, 51.6, 37.1, 24.5, 11.0. IR (cm^{-1}): 3154, 3118, 2971, 2882, 2223, 1572, 1458, 1168, 931. ESI-MS (CH_3CN) (m/z), positive ion: 125 [cation]. Negative ion: 115 $[\text{B}(\text{CN})_4]^-$. Anal. Calcd for $\text{C}_{11}\text{H}_{13}\text{BN}_6$ (240.07): C, 55.03; H, 5.46; N, 35.01%. Found: C, 55.09; H, 5.66; N, 34.98%.

2a: This IL was prepared from N-propyl-pyridinium iodide (2.49 g, 0.01 mol) and $\text{Na}[\text{C}(\text{CN})_3]$ (1.13 g, 0.01 mol) using the same procedure as described above. Yield: 98%. ^1H NMR (Neat, C_6D_6 capillary): 9.25 (d, 2H), 8.90 (dd, 1H), 8.42 (d, 2H), 4.95 (t, 2H), 2.35 (m, 2H), 1.25 (t, 3H). ^{13}C NMR (neat, C_6D_6 capillary): 146.5, 145.5, 130.0, 121.6, 64.0, 31.0, 25.5, 11.0, 6.0. IR (cm^{-1}): 3064, 2971, 2153, 1636, 1488, 1227, 1171, 1066. ESI-MS (CH_3CN) (m/z), positive ion: 122 [cation]⁺. Negative ion: 90 [anion]⁻. Anal. Calcd for $\text{C}_{12}\text{H}_{12}\text{N}_4$ (212.25): C, 67.91; H, 5.70; N, 26.40%. Found: C, 67.88; H, 5.68; N, 26.38%.

2b: This IL was prepared from N-propyl-pyridinium iodide (1.25 g, 0.005 mol) and $\text{K}[\text{B}(\text{CN})_4]$ (0.77 g, 0.005 mol) using the same procedure as described above. Yield: 97%. ^1H NMR (neat, C_6D_6 capillary): 9.25 (d, 2H), 9.00 (dd, 1H), 8.52 (d, 2H), 5.05 (t, 2H), 2.65 (m, 2H), 1.50 (t, 3H). ^{13}C NMR (neat, C_6D_6 capillary): 146.5, 145.5, 130.1, 122.4, 64.5, 25.5, 11.5. IR (cm^{-1}): 3070, 2972, 2222, 1637,

1488, 1173, 1066, 933. ESI-MS (CH_3CN) (m/z), positive ion: 122 [cation]⁺. Negative ion: 115 [B(CN)₄]⁻. Anal. Calcd for C₁₂H₁₂BN₅ (237.07): C, 60.80; H, 5.10; N, 29.54%. Found: C, 60.88; H, 5.11; N, 29.52%.

3a: This IL was prepared from N-propyl-N-methylpyrrolidinium chloride (1.64 g, 0.01 mol) and Na[C(CN)₃] (1.13 g, 0.01 mol) using the same procedure as described above. Yield: 95%. ¹H NMR (neat, C₆D₆ capillary): 3.47 (m, 4H), 3.21 (t, 2H), 3.00 (s, 3H), 2.27 (m, 4H), 1.82 (m, 2H), 1.06 (t, 3H). ¹³C NMR (neat, C₆D₆ capillary): 121.8, 66.2, 65.5, 53.8, 21.7, 17.3, 10.5. IR (cm⁻¹): 2972, 2158, 1470, 1229, 1065, 938, 892. ESI-MS (CH_3CN) (m/z), positive ion: 128 [cation]⁺. Negative ion: 90 [anion]⁻. Anal. Calcd for C₁₂H₁₈N₄ (218.30): C, 66.02; H, 8.31; N, 25.67%. Found: C, 66.28; H, 8.40; N, 25.62%.

3b: This IL was prepared from N-propyl-N-methylpyrrolidinium chloride (1.30 g, 0.008 mol) and K[B(CN)₄] (1.23 g, 0.008 mol) using the same procedure as described above. Yield: 95%, Mp. = 78 °C. ¹H NMR (CH₂Cl₂): 3.65 (m, 4H), 3.30 (t, 2H), 3.05 (s, 3H), 2.30 (m, 4H), 1.90 (m, 2H), 1.10 (t, 3H). ¹³C NMR (CH₂D₂): 122.8, 67.0, 66.5, 49.5, 22.5, 18.0, 10.5. IR (cm⁻¹): 2983, 2887, 2223, 1462, 1307, 1001, 970, 926. ESI-MS (CH_3CN) (m/z), positive ion: 128 [cation]⁺. Negative ion: 115 [B(CN)₄]⁻. Anal. Calcd for C₁₂H₁₈BN₅ (243.12): C, 59.28; H, 7.46; N, 28.81%. Found: C, 59.38; H, 7.60; N, 28.62%.

4a: This IL was prepared from triethylpropyleammonium iodide (2.71 g, 0.01 mol) and Na[C(CN)₃] (1.13 g, 0.01 mol) using the same procedure as described above. Yield: 94%. ¹H NMR (neat, C₆D₆ capillary): 3.65 (q, 6H), 3.45 (q, 2H), 2.05 (m, 2H), 1.65 (t, 9H), 1.35 (t, 3H). ¹³C NMR (neat, C₆D₆ capillary): 121.4, 59.2, 53.2, 15.7, 11.0, 7.8, 5.9. IR (cm⁻¹): 2987, 2901, 2156, 1486, 1456, 1229, 1056, 892. ESI-MS (CH_3CN) (m/z), positive ion: 144 [cation]⁺. Negative ion: 90 [anion]⁻. Anal. Calcd for C₁₃H₂₂N₄ (234.34): C, 66.63; H, 9.46; N, 23.91%. Found: C, 66.68; H, 9.48; N, 23.88%.

4b: This IL was prepared from triethylpropyleammonium iodide (1.36 g, 0.005 mol) and K[B(CN)₄] (0.77 g, 0.005 mol) using the same procedure as described above. Yield: 93%, Mp. = 95 °C. ¹H NMR (CH₂Cl₂): 3.30 (q, 6H), 3.10 (q, 2H), 1.75 (m, 2H), 1.45 (t, 9H), 1.15 (t, 3H). ¹³C NMR (CH₂D₂): 122.6, 59.2, 52.8, 16.0, 11.5, 8.2. IR (cm⁻¹): 2991, 2954, 2223, 1488, 1445, 1392, 1360, 1167, 1086, 998, 927, 800, 789. ESI-MS (CH_3CN) (m/z), positive ion: 144 [cation]⁺. Negative ion: 115 [B(CN)₄]⁻. Anal. Calcd for C₁₃H₂₂BN₅ (259.16): C, 60.25; H, 8.56; N, 27.02%. Found: C, 60.28; H, 8.60; N, 27.12%.

Crystallography. Crystals suitable for X-ray diffraction studies of **3b** and **4b** were obtained by slow cooling of the neat IL, **3b** and **4b**, from 110 °C to room temperature over 24 h. Data collection was performed on a KUMA CCD using graphite-monochromated Mo K α (0.71073 Å) radiation and a low temperature device [$T = 140(2)$ K]. Data reduction was performed using CrysAlis RED.³⁹ The structure was solved with SHELX97.⁴⁰ Refinement was performed using the SHELX97 software package, and graphical representations of the structures were made with Diamond.⁴¹ All structure was solved by direct methods and successive interpretation of the difference Fourier maps, followed by full matrix least-squares refinement (against F^2). All non-hydrogen atoms were refined anisotropically. The contribution of the hydrogen atoms, in their calculated positions, was included in the refinement using a riding model. Relevant details for the structure refinements of **3b** and **4b** are listed in Table 4.

Electrolyte Preparation. A state of the art eutectic ionic-liquid-based electrolyte¹² was used as a model for further modifications. It comprises 1,3-dimethylimidazolium iodide ([DMI][I])/1-ethyl-3-methylimidazolium iodide ([EMI][I])/1-ethyl-3-methylimidazolium tetracyanoborate ([EMI][B(CN)₄])/iodine/*N*-butylbenzimidazole/guanidinium thiocyanate (6:6:8:0.83:1.67:0.33). For the purpose of this study, [EMI][B(CN)₄] in the above-mentioned electrolyte was replaced at the same molar ratio by each of the synthesized ILs: **1a/b**, **2a/b**, **3a**, and **4a**, thus forming six new electrolytes coded as M- (respective IL code).

Viscosity. Viscosity measurements of new modified electrolytes were determined using a HAAKE RheoStress 1 Rheometer (Thermo Scientific) with a HAAKE DCS0 Thermostat (Thermo Scientific).

Table 4. Crystal Data and Structure Refinement Details for **3b and **4b****

| empirical formula | C ₁₂ H ₁₈ BN ₅ (3b) | C ₁₃ H ₂₂ BN ₅ (4b) |
|--|---|---|
| fw | 243.12 | 259.17 |
| temp (K) | 140(2) K | 140(2) |
| cryst size (mm ³) | 0.32 × 0.22 × 0.17 | 0.23 × 0.20 × 0.11 |
| cryst syst | monoclinic | tetragonal |
| space group | <i>P</i> 2 ₁ / <i>c</i> | <i>P</i> 4 ₂ (1) <i>m</i> |
| <i>a</i> (Å) | 8.5730(17) | 11.9402(9) |
| <i>b</i> (Å) | 16.777(3) | 11.9402(9) |
| <i>c</i> (Å) | 9.822(2) | 5.5735(11) |
| β (deg) | 94.74(3) | |
| <i>V</i> (Å ³) | 1407.9(5) | 794.60(18) |
| <i>Z</i> | 4 | 2 |
| <i>D</i> _{calcd} (g·cm ⁻³) | 1.147 | 1.083 |
| <i>F</i> (000) | 520 | 280 |
| abs coeff. (mm ⁻¹) | 0.072 | 0.067 |
| θ range (deg) | 2.38–24.50° | 3.41–25.98 |
| <i>h</i> / <i>k</i> / <i>l</i> | –9,9/–19,19/0,11 | –14,14/–14,14/–6,6 |
| reflns collected | 2301 | 6902 |
| ind reflns | 2301 [<i>R</i> _{int} = 0.0] | 6902 [<i>R</i> _{int} = 0.0447] |
| obsd reflns | 1502 | 709 |
| data/restraints/params | 2301/0/165 | 833/0/57 |
| goodness-of-fit on <i>F</i> ² | 1.175 | 1.095 |
| <i>R</i> , <i>wR</i> indices [<i>I</i> > 2 σ (<i>I</i>)] | 0.0796, 0.2079 | 0.0494, 0.1142 |
| <i>R</i> , <i>wR</i> indices (all data) | 0.1225, 0.2315 | 0.0583, 0.1175 |
| largest diff. peak and hole (e·Å ⁻³) | 0.225, –0.257 | 0.141, –0.107 |

Experiments and data acquisition were supported by the HAAKE RheoWin software. A Ti cone of a diameter of 20 mm and an angle of 0.5° was used for all experiments. Samples were measured at 20 °C. The applied shear rate was in the range 10–8000 s⁻¹ for electrolytes (10–2000 s⁻¹ for pure ILs), and an equilibration time of 30 s was used for each point. In order to obtain the values, a straight line was fitted to a plateau in the low shear rate region for each plot. A point for lowest applied shear rate (10 s⁻¹) was neglected due to the applied measurement procedure.

Device Fabrication. Photoanodes used to make the devices consisted of a screen-printed nanoparticulate mesoporous TiO₂ layers. A 8- μ m-thick transparent layer of 20-nm-sized TiO₂ particles was first printed on the fluorine doped SnO₂ (FTO) conducting glass (NSG-10 Ω /cm², 4-mm-thick) and subsequently coated with a 5- μ m-thick second layer of 400 nm light-scattering anatase particles (CCIC, Japan). Detailed procedures for the preparation of TiO₂ nanoparticles and pastes are reported elsewhere.⁴² A standard Z907 dye was used as the sensitizer with an addition of phenylpropionic acid as a coadsorbent (1:1 ratio) in a solvent mixture of *tert*-butanol and acetonitrile (1:1 v/v ratio). The above-described double-layered TiO₂ films were burnt for 30 min at 500 °C and immersed in the dye solution for 16 h. After sensitization, they were rinsed in pure MeCN and assembled with platinumized counterelectrodes. The counterelectrodes were prepared using conducting glass TEC 15 (resistance 15 Ω /cm², 2 mm thick) on which the drop of a solution of hexachloroplatinate acid in *n*-propanol was cast. Thermal platinization occurred while heating the electrodes twice for 15 min at 425 °C in the air. Electrodes were then sealed with a 25- μ m-thick hot-melt film (Surlyn, Dupont) by heating the system at 100 °C. Devices were completed by filling the space between the electrodes with electrolyte through predrilled holes in the counterelectrodes, and the holes were sealed with a Surlyn sheet and a thin glass cover by heating. Finally, metal contacts were placed on both electrodes.

Photovoltaic Measurements. Photovoltaic measurements were performed under simulated Sun irradiance (100 mW cm⁻², equivalent of 1 Sun at air mass global, AM 1.5G, at the surface of the device)

provided by a 450 W xenon light source (Oriel, USA). A Schott K113 Tempax sunlight filter (Präzisions Glas & Optik GmbH, Germany) was used to correct the spectral output of the lamp in the region 350–750 nm. Current–voltage characteristics (in the dark and under illumination) were obtained by applying a forward potential bias and measuring resulting current with a Keithley 2400 digital sourcemeter (Keithley, USA). A metal mask was used to precisely define the irradiated surface area (0.159 cm²). Quantum efficiencies of the cells were measured by a similar data acquisition system. A Gemini-180 double monochromator (Jobin Yvon Ltd., UK) was used to separate and focus the probing wavelength from the white light being shone by a 300 W xenon lamp (ILC Technology, USA). Measurements were conducted within the UV–vis range (350–850 nm, with a 10 nm interval).

Transient Photovoltage Decay Measurements. Transient decays were measured under white light bias with superimposed red light perturbation pulses (both light sources were LEDs). The voltage dynamics were recorded by using a Keithley 2400 source meter. Varying the intensity of white light bias allowed the recombination rate constant (and thus apparent electron lifetime) to be estimated at different open-circuit potentials by controlling the concentration of the free charges in TiO₂. Red perturbation pulses were adjusted to a very low level in order to maintain single-exponential voltage decay.

Electrochemical Measurements. Cyclic voltammetry and electrochemical impedance spectroscopy were used to determine diffusion coefficients of I₃[−] of the electrolytes. The setup consisted of a Potentiostat/Galvanostat Model 273A (EG&G Princeton Applied Research, USA) and a 1250 Frequency Response Analyzer (Solartron Schlumberger, UK) controlled by CorrWare software (v. 3.2). Symmetric cells were employed with a 20-μm-thick layer of electrolyte encapsulated between two identical electrodes (FTO covered conductive glass TEC15 twice platinized with a solution of H₂PtCl₆ in *n*-propanol, at 450 °C for 15 min). A Surlyn ring, which was used to seal the cell, determined the thickness of the electrolyte layer.

■ ASSOCIATED CONTENT

● Supporting Information

Crystallographic data in CIF format. This material is available free of charge via the Internet at <http://pubs.acs.org>.

■ AUTHOR INFORMATION

Corresponding Author

*E-mail: paul.dyson@epfl.ch, shaik.zakeer@epfl.ch.

■ ACKNOWLEDGMENTS

We thank EPFL and Swiss National Science Foundation for financial support. D.-R.Z. thanks the National Natural Science Foundation of China (No. 21171093) for financial support. M.G. thanks the Swiss National Science Foundation for the financial support under the Indo Swiss Joint Research Programme (ISJRP) grant. We thank Lonza AG for providing Na[C(CN)₃] and Dr. Emil F. Aust, Merck KGaA, Germany for providing us with a sample of K[B(CN)₄]. We also thank Mr. Pascal Comte for providing us the mesoporous TiO₂ films.

■ REFERENCES

- (1) (a) Seddon, K. R. *J. Chem. Technol. Biotechnol.* **1997**, *68*, 351. (b) Welton, T. *Chem. Rev.* **1999**, *99*, 2071. (c) Wasserscheid, P.; Keim, W. *Angew. Chem., Int. Ed.* **2000**, *39*, 3772.
- (2) (a) Dyson, P. J. *Appl. Organomet. Chem.* **2002**, *16*, 495. (b) Dupont, J.; De Souza, R. F.; Suarez, P. A. Z. *Chem. Rev.* **2002**, *102*, 3667. (c) Ciappe, C.; Pieraccini, D. *J. Phys. Org. Chem.* **2005**, *18*, 275. (d) Fei, Z.; Geldbach, T. J.; Zhao, D.; Dyson, P. J. *Chem.—Eur. J.* **2006**, *12*, 2122. (e) Migowski, P.; Dupont, J. *Chem.—Eur. J.* **2007**, *13*, 32.
- (3) Xue, H.; Verma, R.; Shreeve, J. M. *J. Fluorine Chem.* **2006**, *127*, 159.
- (4) Yoshida, Y.; Muroi, K.; Otsuka, A.; Saito, G.; Takahashi, M.; Yoko, T. *Inorg. Chem.* **2004**, *43*, 1458.
- (5) Wang, P.; Wenger, B.; Humphry-Baker, R.; Moser, J.-E.; Teuscher, J.; Kantelehner, W.; Mezger, J.; Stoyanov, E. V.; Zakeeruddin, S. M.; Grätzel, M. *J. Am. Chem. Soc.* **2005**, *127*, 6850.
- (6) Wang, P.; Zakeeruddin, S. M.; Grätzel, M.; Kantelehner, W.; Mezger, J.; Stoyanov, E. V.; Scherr, O. *Appl. Phys. A: Mater. Sci. Process.* **2004**, *79*, 73.
- (7) Welz-Biermann, U.; Ignatyev, N.; Bernhardt, E.; Finze, M.; Willner, H. Merck GmbH, Darmstadt, Germany; Patent WO 2004/072089 A1, 2004.
- (8) Kuang, D.; Wang, P.; Ito, S.; Zakeeruddin, S. M.; Grätzel, M. *J. Am. Chem. Soc.* **2006**, *128*, 7732.
- (9) (a) Huddleston, J. G.; Visser, A. E.; Reichert, W. M.; Willauer, H. D.; Broker, G. A.; Rogers, R. D. *Green Chem.* **2001**, *3*, 156. (b) McEwen, A. B.; Ngo, H. L.; LeCompte, K.; Goldman, J. L. *J. Electrochem. Soc.* **1999**, *146*, 1687.
- (10) Tong, J.; Liu, Q.-S.; Kong, Y.-X.; Fang, D.-W.; Welz-Biermann, U.; Yang, J.-Z. *J. Chem. Eng. Data* **2010**, *55*, 3693.
- (11) Kuang, D.; Uchida, S.; Humphry-Baker, R.; Zakeeruddin, S. M.; Graetzel, M. *Angew. Chem., Int. Ed.* **2008**, *47*, 1923.
- (12) Bai, Y.; Cao, Y.; Zhang, J.; Wang, M.; Li, R.; Wang, P.; Zakeeruddin, S. M.; Graetzel, M. *Nat. Mater.* **2008**, *7*, 626.
- (13) Kuang, D.; Klein, C.; Zhang, Z.; Ito, S.; Moser, J.-E.; S. Zakeeruddin, S. M.; Graetzel, M. *Small* **2007**, *3*, 2094.
- (14) Lei, Z.; Chen, B.; Li, C. *Chem. Eng. Sci.* **2007**, *62*, 3940.
- (15) Yan, P. F.; Yang, M.; Liu, X.-M.; Wang, C.; Tan, Z.-C.; Welz-Biermann, U. *J. Chem. Thermodyn.* **2010**, *42*, 817.
- (16) (a) Wilkes, J. S.; Zaworotko, M. J. *Chem. Commun.* **1992**, 965. (b) Suarez, P. A. Z.; Dullius, J. E. L.; Einloft, S.; de Souza, R. F.; Dupont, J. *Polyhedron* **1996**, *15*, 1217.
- (17) Bonhote, P.; Dias, A.-P.; Papageorgiou, N.; Kalyanasundaram, K.; Graetzel, M. *Inorg. Chem.* **1996**, *35*, 1168.
- (18) Mazille, F.; Fei, Z.; Kuang, D.; Zhao, D.; Zakeeruddin, S. M.; Grätzel, M.; Dyson, P. J. *Inorg. Chem.* **2006**, *45*, 1585.
- (19) Fei, Z.; Kuang, D.; Zhao, D.; Klein, C.; Ang, W. H.; Zakeeruddin, S. M.; Grätzel, M.; Dyson, P. J. *Inorg. Chem.* **2006**, *45*, 1047.
- (20) Brand, H.; Liebman, J. F.; Schulz, A.; Mayer, P.; Villinger, A. *Eur. J. Inorg. Chem.* **2006**, 4294.
- (21) Enemark, H.; Holm, R. H. *Inorg. Chem.* **1964**, *3*, 1516.
- (22) Miller, F. A.; Baer, W. K. *Spectrochim.* **1963**, *19*, 73.
- (23) Andersen, P.; Klewe, B.; Thom, E. *Acta Chem. Scand.* **1967**, *21*, 1530.
- (24) Witt, J.; Britton, D. *Acta Crystallogr.* **1971**, *B27*, 1835.
- (25) Küppers, T.; Bernhardt, E.; Willner, H.; Rohm, H. W.; Köckerling, M. *Inorg. Chem.* **2005**, *44*, 1015.
- (26) Neukirch, M.; Tragl, S.; Meyera, H.-J.; Küppers, T.; Willner, H. *Z. Anorg. Allg. Chem.* **2006**, *632*, 939.
- (27) Nitschke, C.; Köckerling, M. *Z. Anorg. Allg. Chem.* **2009**, *635*, 503.
- (28) Bernhardt, E.; Henkel, G.; Willner, H. *Z. Anorg. Allg. Chem.* **2000**, *626*, 560.
- (29) Flemming, A.; Hoffmann, M.; Köckerling, M. *Z. Anorg. Allg. Chem.* **2010**, *636*, 562.
- (30) Bessler, E.; Goubeau, J. *Z. Anorg. Allg. Chem.* **1967**, *352*, 67.
- (31) Williams, D.; Pleune, B.; Kouvetakis, J.; Williams, M. D.; Andersen, R. A. *J. Am. Chem. Soc.* **2000**, *122*, 7735.
- (32) Küppers, T.; Köckerling, M.; Willner, H. *Z. Anorg. Allg. Chem.* **2007**, *633*, 280.
- (33) Koppe, K.; Frohn, H.-J.; Mercier, H. P. A.; Schrobilgen, G. J. *Inorg. Chem.* **2008**, *47*, 3205.
- (34) Choudhury, A. R.; Winterton, N.; Steiner, A.; Cooper, A. I.; Johnson, K. A. *J. Am. Chem. Soc.* **2005**, *127*, 16792.
- (35) Choudhury, A. R.; Winterton, N.; Steiner, A.; Cooper, A. I.; Johnson, K. A. *CrystEngComm* **2006**, *8*, 742.
- (36) Hipps, K. W.; Aplin, A. T. *J. Phys. Chem.* **1985**, *89*, 5459.
- (37) Zhang, M.; Zhang, J.; Bai, Y.; Su, M.; Wang, P. *Phys. Chem. Chem. Phys.* **2011**, *13*, 3788.

- (38) (a) Dyson, P. J.; Khalaila, I.; Luetzgen, S.; McIndoe, J. S.; Zhao, D. *Chem. Commun.* **2004**, 2204. (b) Dyson, P. J.; McIndoe, J. S.; Zhao, D. *Chem. Commun.* **2003**, 508.
- (39) Duisenberg, A. J. M.; Kroon-Batenburg, L. M. J.; Schreurs, A. M. *M. J. Appl. Crystallogr.* **2003**, 36, 220.
- (40) Sheldrick, G. M. *SHELX-97*; Universität Göttingen: Göttingen, Germany, 1997.
- (41) Farrugia, L. J. *J. Appl. Crystallogr.* **1997**, 30, 565.
- (42) Ito, S.; Chen, P.; Comte, P.; Nazeeruddin, M. K.; Liska, P.; Péchy, P.; Grätzel, M. *Prog. Photovolt. Res. Appl.* **2007**, 15, 603.